

Isoform-specific Binding of Selenoprotein P to the β -Propeller Domain of Apolipoprotein E Receptor 2 Mediates Selenium Supply*

Received for publication, January 8, 2014, and in revised form, February 10, 2014. Published, JBC Papers in Press, February 13, 2014, DOI 10.1074/jbc.M114.549014

Suguru Kurokawa^{†1}, Frederick P. Bellinger[‡], Kristina E. Hill[§], Raymond F. Burk[§], and Marla J. Berry[‡]

From the [‡]Department of Cell and Molecular Biology, John A. Burns School of Medicine, University of Hawaii, Honolulu, Hawaii 96813 and the [§]Division of Gastroenterology, Hepatology, and Nutrition, Department of Medicine, Vanderbilt University School of Medicine, Nashville, Tennessee 37232

Background: ApoER2 facilitates uptake of Sepp1, but the binding mechanism has not been elucidated.

Results: The two longest isoforms of Sepp1 bind to the YWTD β -propeller domain of apoER2, which functions as a Sepp1 receptor.

Conclusion: Only longer Sepp1 isoforms with six or more selenocysteine residues can interact with a unique binding site of apoER2.

Significance: ApoER2 takes up long isoform Sepp1 through its YWTD β -propeller domain.

Sepp1 supplies selenium to tissues via receptor-mediated endocytosis. Mice, rats, and humans have 10 selenocysteines in Sepp1, which are incorporated via recoding of the stop codon, UGA. Four isoforms of rat Sepp1 have been identified, including full-length Sepp1 and three others, which terminate at the second, third, and seventh UGA codons. Previous studies have shown that the longer Sepp1 isoforms bind to the low density lipoprotein receptor apoER2, but the mechanism remains unclear. To identify the essential residues for apoER2 binding, an *in vitro* Sepp1 binding assay was developed using different Sec to Cys substituted variants of Sepp1 produced in HEK293T cells. ApoER2 was found to bind the two longest isoforms. These results suggest that Sepp1 isoforms with six or more selenocysteines are taken up by apoER2. Furthermore, the C-terminal domain of Sepp1 alone can bind to apoER2. These results indicate that apoER2 binds to the Sepp1 C-terminal domain and does not require the heparin-binding site, which is located in the N-terminal domain. Site-directed mutagenesis identified three residues of Sepp1 that are necessary for apoER2 binding. Sequential deletion of extracellular domains of apoER2 surprisingly identified the YWTD β -propeller domain as the Sepp1 binding site. Finally, we show that apoER2 missing the ligand-binding repeat region, which can result from cleavage at a furin cleavage site present in some apoER2 isoforms, can act as a receptor for Sepp1. Thus, longer isoforms of Sepp1 with high selenium content interact with a binding site distinct from the ligand-binding domain of apoER2 for selenium delivery.

Selenium is an essential micronutrient, because of its presence in selenoproteins in the form of selenocysteine. Humans

have 25 selenoproteins, and rodents have 24 (1). Selenocysteine is encoded by UGA codons, which also serve as stop codons. UGA codons in the open reading frame of selenoprotein mRNAs are decoded by a selenocysteine insertion (SECIS)² element in the 3'-untranslated region in eukaryotes (2). Selenocysteine is synthesized on a unique tRNA, tRNA^{[Ser]Sec}, which recognizes the UGA stop codon to recode for selenocysteine insertion. SECIS elements recruit a specific RNA-binding protein termed SECIS binding protein 2 (SBP2), which in turn recruits the selenocysteyl-tRNA^{[Ser]Sec} bound by a specific elongation factor, eEFSec. This complex delivers the charged tRNA to the ribosome, facilitating the translation of selenoproteins (3). SECIS elements have differing efficiency for selenocysteine incorporation (4). Further, selenoprotein mRNAs exhibit differing responses to selenium status, with some selenoprotein mRNAs being dramatically decreased under conditions of selenium deficiency compared with selenium adequacy. In contrast, other selenoprotein mRNAs are minimally affected by selenium status. Thus, selenoprotein expression is regulated in a multistep process, generating a hierarchy of selenoproteins. The hierarchy demonstrates regulation under conditions of limiting selenium to redistribute selenium to the selenoproteins with the highest demand in the cell. In addition, tissue selenium distribution also follows a hierarchy, with some tissues such as brain and testes having better retention of selenium under low selenium conditions (4, 5).

Selenoprotein P (Sepp1) is an extracellular glycoprotein that has multiple selenocysteine residues and functions as a selenium transport protein via receptor-mediated endocytosis (5, 6). Sepp1 mRNA is present in most tissues, and hepatocytes produce large quantities and export Sepp1 protein into plasma, where it accounts for ~60% of plasma selenium (7). The N-ter-

* This work was supported, in whole or in part, by National Institutes of Health Grants DK047320 and G12 MD007601 (to M. J. B.).

[†] To whom correspondence should be addressed: Dept. of Cell and Molecular Biology, John A. Burns School of Medicine, University of Hawaii, 651 Ilalo St., Honolulu, HI 96813. Tel.: 808-692-1773; Fax: 808-692-1970; E-mail: kurokawasuguru@gmail.com.

² The abbreviations used are: SECIS, selenocysteine insertion sequence; apoER2, apolipoprotein E receptor-2; Gpx, glutathione peroxidase; H-rich, histidine-rich; LBR, ligand binding repeat; PBS, phosphate-buffered saline; RAP, low density lipoprotein receptor-related protein-associated protein 1; Sepp1, selenoprotein P; U and Se-Cys, selenocysteine.

Selenoprotein P and Apolipoprotein E Receptor-2 Interaction

minal and C-terminal domains of Sepp1 are proposed to have distinct functions (8). Mouse, rat, and human Sepp1 have ten selenocysteine residues, one within the N-terminal domain and nine in the C-terminal domain. The first selenocysteine residue in the N-terminal domain forms the redox motif UXXC (where U indicates selenocysteine), which is a functional redox domain with thioredoxin-like properties. The selenium-rich C terminus has been demonstrated to supply selenium to tissues (9). Sepp1 has a heparin-binding site in the N-terminal domain (10), which facilitates Sepp1 uptake by cells. Two histidine-rich (H-rich) domains likely contribute to the heparin binding properties of Sepp1 (10).

Immunoaffinity-purified rat plasma Sepp1 is present as a full-length protein and three shorter isoforms, which terminate at the positions of the second, third, and seventh selenocysteine residues (11). The three shorter isoforms thus contain reduced selenium content, *i.e.*, one, two, and six selenocysteine residues, respectively. Because the identified isoforms terminate at the UGA codon for selenocysteine, isoforms of Sepp1 are likely regulated by competing translation elongation and termination (12, 13).

Deletion of Sepp1 moderately decreases whole body selenium (14, 15). Brain and testis retain selenium under low dietary selenium conditions, but not when Sepp1 is deleted. This indicates that Sepp1 supplies selenium preferentially to these tissues when selenium intake is restricted. Apolipoprotein E receptor 2 (apoER2) and megalin, members of the low density lipoprotein receptor family, have been identified as Sepp1 receptors, which facilitate Sepp1 endocytosis and maintain selenium homeostasis (6, 16). ApoER2 is highly expressed in testis Sertoli cells, and apoER2 knock-out mice showed reduced male fertility because of defective spermatozoa (17). This is largely due to reduced production of the selenoprotein glutathione peroxidase 4, which serves as a structural component of the sperm mitochondrial capsule, a specialized structure associated with the outer mitochondrial membrane of spermatozoa (18). The male infertility phenotype of apoER2 knock-out mice is similar to that of Sepp1 knock-out mice (19). ApoER2 is also expressed in placenta (20). Recent studies demonstrated that fetal apoER2 binds maternal Sepp1 in the day 18 mouse placenta (21). Thus, apoER2-mediated Sepp1 transport is important for fetal development. On the other hand, megalin is responsible for Sepp1 uptake on the brush border of renal proximal convoluted tubule cells (16). Previously, a C-terminal deletion Sepp1 strain (Sepp1^{Δ240–361}) was produced to characterize the domain function of Sepp1 *in vivo* (9). Several studies using immunostaining have shown that testis apoER2 does not bind Sepp1^{Δ240–361}. However, Sepp1^{Δ240–361} was detected in kidney, which only expresses megalin (16). Furthermore, a recent study identified N-terminal Sepp1 fragments in megalin knock-out mouse urine (22). These results suggest that apoER2 and megalin have different ligand binding properties for Sepp1. It is thus postulated that apoER2 is selective for longer Sepp1 isoforms to maximize selenium uptake by tissues, whereas megalin prevents the loss of Sepp1 in the urine by binding N-terminal Sepp1 (23). Furthermore, apoER2 has signaling functions in the brain that are activated by its ligand, reelin, and are not dependent on endocytosis of ligand (24). Recently, a study uti-

lizing apoER2 knock-in mice with altered cytoplasmic tails demonstrated involvement of apoER2 in spermatogenesis, likely because of Sepp1 and/or selenium trafficking (25). Sepp1 putatively binds the extracellular region of apoER2, which consists of ligand binding repeats (LBRs), the epidermal growth factor repeat, the YWTD β -propeller domain, and the O-linked sugar domain. Reelin and other well characterized ligands have been shown to bind the LBRs (26–28).

It is currently not known which domain of apoER2 recognizes Sepp1 and which isoforms of Sepp1 are ligands for apoER2. In this study, we investigated the potential apoER2 binding residues in Sepp1 and demonstrate that only the longer two isoforms can bind apoER2 via the Sepp1 C-terminal domain. Thus, apoER2 takes up Sepp1 isoforms with six or more selenocysteine residues. Further, we confirmed that the C-terminal domain binds to apoER2. We also investigated potential Sepp1 binding regions of apoER2. Unexpectedly, we found that Sepp1 binds to the β -propeller domain of apoER2. We further demonstrate that apoER2 lacking the LBR can still function as a Sepp1 receptor, suggesting a unique mechanism of receptor-dependent endocytosis of Sepp1.

EXPERIMENTAL PROCEDURES

Materials—All reagents were purchased from Sigma-Aldrich, unless otherwise noted. The human embryonic kidney 293T (HEK293T) cell line was purchased from the American Type Culture Collection (Manassas, VA). Mouse Sepp1 expression clone (pCMV-Sepp1) was purchased from OriGene Technologies (Rockville, MD). The expression plasmid for GFP-fused mouse apoER2 was a generous gift from Prof. Mitsuharu Hattori (Nagoya City University, Nagoya, Japan) (26). The expression plasmid for polyhistidine-fused low density lipoprotein receptor-associated protein (RAP) was a generous gift from Prof. Toshimi Michigami (Osaka Medical Center and Research Institute for Maternal and Child Health, Osaka, Japan). The purification scheme for RAP protein was previously described (27). RAP protein was purified to homogeneity, and its purity was evaluated by SDS-PAGE. Proteinase inhibitor mixture was purchased from EMD Millipore (Billerica, MA). Criterion TGX gels, protein markers, and SDS sample buffer were purchased from Bio-Rad. The rabbit polyclonal Sepp1 antibody against the N-terminal region from mouse Sepp1 was described previously (28). Rabbit anti-apoER2 and mouse anti- β -actin antibodies were purchased from Sigma-Aldrich. Rabbit Anti-GFP and mouse anti-V5 antibodies were purchased from Invitrogen. Goat anti-Gpx1 antibodies were purchased from R&D Systems (Minneapolis, MN). All commercial antibodies used were diluted according to the manufacturer's protocols. EGFP expression plasmid (pEGFP-N1) was purchased from Clontech. Polyethyleneimine, linear (molecular weight, 250,000) was purchased from Polysciences, Inc. (Warrington, PA). All oligonucleotides were synthesized by Integrated DNA Technologies (Coralville, IA). Phusion-polymerase and all reagents for DNA modification were purchased from New England Biolabs (Ipswich, MA). Other chemicals were reagent grade or better.

Animals—These studies used sera from mice with deleted or altered Sepp1. Sepp1^{+/+} or Sepp1^{-/-} sera were obtained from the corresponding mice housed in the University of Hawaii

TABLE 1
PCR primers for plasmid construction

Plasmid	Primer designation	Primer sequence (5' → 3')
Sepp1 U2C	mSepp1U259CF	GTCACCTAGAGAGCTGTGACACCACGCAAGTG
	mSepp1U259CR	CACTTGCTGTGGTGTACACGCTCTTAAGTGAC
Sepp1 U3C	mSepp1U277CF	GCCCAGAGGGCCCTCTGTGCAAGGGGGTGCATC
	mSepp1U277CR	GATGCACCCCTTCGACAGAGGGCCCTCTGGGC
Sepp1 U4C	mSepp1U318CF	GGTCTGCAATTGCTTGTGTCAGTGTGCGGAAAAC
	mSepp1U318CR	GTTTTCCGCACACTGACAAGCAATTGCAGACCC
Sepp1 U5C	mSepp1U330CF	CCATCCTTATGTAGCTGCCAGGGGCTTTTCGCG
	mSepp1U330CR	CGCGAAAAGCCCTGGCAGCTACATAAGGATGG
Sepp1 U6C	mSepp1U352CF	TCACCTCCAGCTGCCTGCCAAAATCAGCCCATG
	mSepp1U352CR	CATGGGCTGATTTGGCAGGCAGCTGGAGGTGA
Sepp1 U7–8C	mSepp1U352CF	GCCAACCCCAACTGTAGCTGTGATAATCAGACC
	mSepp1U352CR	GGTCTGATTATCAGCTACAGTGTGGGTTGGC
Sepp1 U9–10C	mSepp1U352CF	CAGACCAGGAAGTGTAAATGTCATTCAAAC
	mSepp1U352CR	GTTTGAATGACATTTACACTTCTCGGTCTG
Sepp1 1–322	mSepp1 1–322R	TTCAAGTGACTTTCTCCTCCGC
Sepp1 1–323	mSepp1 1–323R	GGATTCAGTGACTTTCTCCTC
Sepp1 1–324	mSepp1 1–324R	ACAGGATTCAGTGACTTTCTC
Sepp1 1–325	mSepp1 1–325R	CTGACAGGATTCAGTGACTTT
Sepp1 1–326	mSepp1 1–326R	ACACTGACAGGATTCAGTGAC
Sepp1 1–327	mSepp1 1–327R	CCTACACTGACAGGATTCAGT
Sepp1 S323A	Sepp1 S323AR	ACACTGACAGGCTTCAGTGACTCCCTCCTCCGC
Sepp1 C324A	Sepp1 C324AR	ACACTGACAGGATTCAGTGACTCCCTCCTCCGC
Sepp1 Q325A	Sepp1 Q325AR	ACACGCACAGGATTCAGTGACTCCCTCCTCCGC
Sepp1 C326A	Sepp1 C326AR	AGCCTGACAGGATTCAGTGACTCCCTCCTCCGC
GFP-Sepp1	NheI EGFPF	CTAGCTAGCATGGTGTAGCAAGGGC
	BamHI EGFPF	CGCGGATCCCTTGTACAGCTCGTC
GFP-Sepp1 187–361	SeP187-CBamHIF	ACGGGATCCCAACCAACACCAAC
GFP-Sepp1 208–361	Sep208-CBamHIF	ACGGGATCCCAAGCAAGGGCCATCAG
apoER2 dLBR	mApoER2 dLBRF	CTGCCGGGGCGCCAAAGGGTAAATGAGTGTCTG
	mApoER2 dLBRR	CAGACACTCATTTAGCCCTTTGGCCCGCCGGCAG
apoER2 dAB	mApoER2 dAB F	CTGCCGGGGCGCCAAAGAGCCCATCTCTGA
	mApoER2 dAB R	TCAGAGATGGGCTCTTTTGGCCCGCCGGCAG
apoER2 dBP	mApoER2 dBP F	CTGCCGGGGCGCCAAAGCAGATGCCTGTGAC
	mApoER2 dBP R	GTACACAGGCATCTGCTTGGCCCGCCGGCAG
apoER2 dC	mApoER2 dC F	CTGCCGGGGCGCCAAACAGTCTACTCAACT
	mApoER2 dC R	AGTTGAGGTAGACTGTGGCCCGCCGGCAG
apoER2 dO	mApoER2 dO F	CTGCCGGGGCGCCAAACATATGGGAATGAA
	mApoER2 dO R	TTCAATCCCATAAATGTGGCCCGCCGGCAG
apoER2 dBP2	mApoER2 dBP2 F	TGCAAAGCTGTAGCCGAGATGCCTGTGAC
	mApoER2 dBP2 R	TGCAAAGCTGTAGCC

vivarium. Sepp1^{Δ240–361} serum was collected at Vanderbilt University. The mice were housed in the Vanderbilt University or the University of Hawaii vivariums, with 12-h light/12-h dark cycles. They were fed a Torula yeast-based diet that contained 0.25 mg of selenium/kg (29). Food and tap water were provided *ad libitum*. Care and use of animals in these experiments conformed to National Institutes of Health guidelines for animal care and use in research. The Institutional Animal Care and Use Committee of the University of Hawaii approved all animal protocols. Placentae were obtained from mice in late pregnancy (15 days gestation). Testes were obtained from a 3-month-old animal.

Plasmids—The sequential deletion plasmids for GFP fusion mouse apoER2 proteins were constructed using site-directed mutagenesis techniques. All amplified PCR fragments were generated using Phusion-polymerase. TGA codons for selenocysteines were mutated to TGT (Se-Cys^{1–4} and Se-Cys^{7–10}) or TGC (Se-Cys⁵ and Se-Cys⁶), respectively. Primer sequences for plasmid preparation are given in Table 1. The expression plasmid for V5 epitope-fused mouse Sepp1 was constructed by introducing a V5 epitope tag after the signal sequence of Sepp1. The sequence of the oligonucleotides for V5 epitope 5'-CTAGCGGTAAGCCTATCCCTAACCCCTCTCCTCGGTC-TCGATTCTACGG-3' and 5'-GATCCCGTAGAATCGAGACCAGGAGAGGGTTAGGGATAGGCTTACCG-3' were annealed and phosphorylated by T4 polynucleotide kinase.

Then pCMV-Sepp1 was amplified by Sepp1NheI (5'-ACCG-CTAGCGCTCTCTGCTCCTCCA-3') and Sepp1BamHIF (5'-ACGGGATCCGAGAGCCAAGGCCAAA-3') primers, respectively. The amplified product was purified and digested with NheI and BamHI and then ligated with the V5 epitope duplex. Site-directed mutagenesis was used to generate cysteine mutants of mouse Sepp1, where UGA codons corresponding to selenocysteine residues were mutated to codons corresponding to cysteine residues. The 3'-UTR was removed using Sepp1SECISdelF (5'-TAATACGACTAAGCAAGAATGGAG-3') and Sepp1U-352CR oligonucleotides. Constructs expressing C-terminal Sepp1 fragments fused to EGFP at the N terminus were made. The sequence of the insert for EGFP was amplified using NheI EGFPF and BamHI EGFPF primers. The fragment was purified and digested with NheI and BamHI and then ligated into pCMV-Sepp1-cys cut with NheI and BamHI. GFP-Sepp1-cys 187–361 and 208–361 were generated with PCR using SeP187-CBamHIF and SeP208-CBamHIF as forward primers. The sequences of all of the fragments amplified by PCR were verified. Further details of the methods and the maps of the plasmids will be supplied on request.

Cell Culture and Transfection—HEK293T cells were cultured in DMEM supplemented with 10% (v/v) FBS, penicillin, streptomycin, and glutamine on Petri dishes or multiwell plates that had been coated with poly-D-lysine, maintained in humidified 95% air, 5% CO₂ at 37 °C. Prior to transfection, cells were

Selenoprotein P and Apolipoprotein E Receptor-2 Interaction

washed three times with PBS and incubated with transfection medium. Transfection with DNA constructs was performed with polyethyleneimine with a few modifications. Briefly, for multiwell plates, transfection medium was prepared by mixing 1:10 (w/w) ratio of DNA to polyethyleneimine in 100 μ l of DMEM and incubated at room temperature for 20 min to form transfection complexes. 500 μ l of DMEM was added to the transfection complexes, and then it was replaced with culture medium. Cells were incubated in humidified 95% air, 5% CO₂ at 37 °C for 4 h, and then transfection medium was replaced with 500 μ l of DMEM supplemented with 10% FBS. Incubation was continued for an additional 2 days. For Sepp1 binding assay, to avoid degradation of the apoER2-GFP fusion protein, HEK293T cells expressing the protein were incubated for no longer than 60 h after the transfection. All Sepp1 binding studies were carried out in medium that did not contain FBS. For assay utilization of selenium from Sepp1, 24 h post-transfection, cells were preincubated for 24 h in serum-free medium. Then culture medium was replaced with fresh DMEM supplemented with 0.2% mouse serum and incubated for an additional 24 h. Cells were rinsed three times with PBS and collected for Gpx1 protein analysis by Western blot.

Preparation of Recombinant Sepp1-cys Conditioned Medium—HEK293T cells (3.5×10^6 /dish) were cultured in 100-mm Petri dishes in 5 ml of culture medium and transfected with Sepp1-cys constructs or negative control plasmid. The following day, the culture medium was replaced with DMEM without serum. After 2 more days, the conditioned medium was collected. The conditioned medium was then centrifuged at $400 \times g$ for 10 min to remove cell debris, and the supernatant was further centrifuged at $20,000 \times g$ for 15 min at 4 °C. The supernatant fraction collected was transferred to 10-kDa Amicon ultracentrifugal units, concentrated to 500 μ l, and stored at -20 °C until use. Twenty μ l of the conditioned medium was analyzed by SDS-PAGE and Western blot.

Sepp1 Binding Studies—HEK293T cells expressing apoER2-GFP or GFP proteins as a negative control were cultured in multiwell dishes. Cells were trypsinized and collected by centrifugation. They were resuspended in culture medium at 3.5×10^5 cells/well in a volume of 500 μ l/well, and transfection was conducted. Forty-eight hours post-transfection, the cells were rinsed with PBS three times and incubated with 500 μ l of DMEM containing 10% mouse serum or recombinant Sepp1-cys conditioned medium for 3 h under humidified 95% air, 5% CO₂ at 37 °C. After incubation, the supernatant was removed, and the cells were washed with DMEM containing 2 mM CaCl₂ three times at 4 °C. Cells were centrifuged at $400 \times g$ for 1 min, and supernatant was removed; then cells were lysed with PBS containing 1% Nonidet P-40, 5 mM EDTA, and proteinase inhibitors on ice. Lysates were sonicated and centrifuged at $20,000 \times g$ for 15 min at 4 °C, and protein supernatant was collected. The amount of Sepp1 protein bound to cells was analyzed by Western blotting. For RAP binding experiments, a final concentration of RAP protein (0.5–2 μ M) was added to fresh DMEM, and cells were preincubated for 15 min under humidified 95% air, 5% CO₂ at 37 °C. Then medium was replaced with fresh DMEM supplemented with RAP protein and 10% mouse serum, and incubation was continued for an additional 3 h

under humidified 95% air, 5% CO₂ at 37 °C. All experiments were performed in duplicate.

Western Blotting—Aliquots of HEK293T cells were resuspended in 50 μ l of ice-cold PBS containing 1% Nonidet P-40 substitute and protease inhibitor mixture, and the lysates were ultrasonicated using a Sonic Dismembrator 100 (Fisher) on power setting 1, with 15-s pulses to shear the genomic DNA. Cell lysate was centrifuged at $20,000 \times g$ for 15 min, and then supernatant was resuspended in SDS loading buffer containing 5% 2-mercaptoethanol, electrophoresed on Protean TGX 4–20% (w/v) polyacrylamide gels, and transferred to Immobilon-FL polyvinylidene difluoride membranes (EMD Millipore, Billerica, MA). After 30 min of blocking, the membranes were incubated with the following primary antibodies: rabbit anti-mouse Sepp1 (1:300), mouse apoER2 (1:300), GFP (1:500), β -actin (1:5000), or mouse anti-V5 (1:500) antibodies. After 1 h of incubation with the corresponding antibodies, the membranes were then washed with Tris-buffered saline with Tween 20 (25 mM Tris/HCl, pH 7.5, 150 mM NaCl, and 0.1% Tween 20) three times. Then corresponding secondary antibodies (diluted 1:10,000) were applied. After 1 h of incubation with corresponding secondary antibodies, the membranes were washed, and the proteins were detected and analyzed by an Odyssey Infrared Imager (Li-Cor Biosciences, Lincoln, NE). To study the time course of Sepp1 degradation, apoER2-overexpressing cells were incubated with 10% mouse serum, washed three times, and then collected at 1, 3, 5, and 7 h. Whole cell lysates were analyzed by Western blot using rabbit anti-Sepp1 antibody as described above.

Affinity Purification of ApoER2 by Sepp1 or RAP from Testis or Placenta—Preparation of mouse plasma Sepp1 using a Sepp1 antibody (9S4) column was described previously (6). Sepp1 or RAP proteins were immobilized on AminoLink coupling resin (Thermo Fisher Scientific Inc., Rockford, IL) at pH 7.4. A previously described membrane preparation was modified for mouse testis or placenta (30). Briefly, tissues were suspended in ice-cold TNI (150 mM NaCl, 25 mM Tris-HCl, pH 7.5, 2 mM benzamide, 1 μ g/ml leupeptin, and 1 μ g/ml pepstatin) and homogenized with a Polytron homogenizer. The suspension was centrifuged at $11,000 \times g$ for 30 min, the supernatant was discarded, and the pellet was washed by resuspension in TNI followed by the same centrifugation conditions as above. Membrane proteins were solubilized at 4 °C in TNI containing 1% Triton X-100, and insoluble material was pelleted with centrifugation as above. CaCl₂ and MgCl₂ were added to the Triton-soluble fractions at 1 mM final concentration and then incubated with the AminoLink coupling resin with bound mouse Sepp1 or RAP. The resin was packed into a column and washed with 10 volumes of TNI. Bound proteins were eluted with 0.1 M glycine-HCl, pH 2.5.

Solid Phase Binding Assay—A previously described solid phase binding assay was modified for mouse Sepp1 and apoER2-GFP (32). Mouse plasma Sepp1 was purified using a 9S4 column. The total protein was measured by Bradford assay, and the molar concentration was calculated assuming the molecular weight of full-length Sepp1 is 40,692. Note that this value will underestimate the molar concentration because plasma Sepp1 is a mixture of isoforms of Sepp1. The prepara-

tion of immobilized anti-GFP antibody AminoLink coupling resin is described above. ApoER2-GFP was overexpressed in HEK293T cells, purified using anti-GFP antibody immobilized to AminoLink coupling resin, and coated (5 nM) on a 96-well plate overnight at 4 °C. Li-Cor blocking buffer was used for blocking and binding of Sepp1 for 1 h at room temperature. 100 μ l of samples containing 0, 1.4, 2.8, 5.6, 11.3, 22.5, 45, 67.5, and 90 nM purified Sepp1 were incubated in triplicate. Unbound Sepp1 was washed three times with TNI buffer containing 0.1% Tween 20. After washing, anti-Sepp1 (1:300) followed by HRP-conjugated secondary antibodies (1:2000) were used for detection of the bound Sepp1. Tetramethyl benzidine solution (Invitrogen) was used for the color reaction. The reaction was stopped after 15 min by addition of 0.1 M H₂SO₄, and the resulting yellow solution was measured at 450 nm.

Statistics—Quantification of Western blot bands was carried out using Image-Studio (Li-Cor Biosciences, Lincoln, NE), and results were plotted and analyzed using Prism software (GraphPad Software Inc., La Jolla, CA). Student's *t* test was used to determine differences in groups. The results are means \pm S.E.

RESULTS

Sepp1 Longer Isoforms Bind to ApoER2, but Shorter Forms Do Not—We evaluated Sepp1 binding to apoER2 *in vitro* using serum Sepp1 from Sepp1^{+/+} or Sepp1 ^{Δ 240–361} transgenic mice. Expression of mouse Sepp1 isoforms was confirmed by Western blot using rabbit anti-Sepp1 antibody (Fig. 1A, left panel). A strong single band of ~50 kDa corresponding with mature glycosylated Sepp1 was detected in mouse serum (lane 1). Sepp1 ^{Δ 240–361} serum showed two bands at ~45 and ~50 kDa (lane 2), possibly representing differentially glycosylated forms of the truncated protein. Sepp1^{-/-} serum showed no detectable bands by Western blot (lane 3).

The right panel of Fig. 1A shows the blot stained with Coomassie Blue. The binding of Sepp1 to apoER2 was assessed by the incubation of mouse serum with apoER2-overexpressing HEK293T cells (Fig. 1B). Mouse sera from Sepp1^{+/+} or Sepp1 ^{Δ 240–361} were loaded as reference for the migration sizes of Sepp1 isoforms (lanes 1 and 2, respectively). GFP as a negative control (lanes 3–5) or apoER2-GFP (lanes 6–8) proteins were overexpressed in HEK293T cells, which were then exposed to culture media containing serum from Sepp1^{+/+} (lanes 5 and 8) or Sepp1 ^{Δ 240–361} (lanes 4 and 7) mice. Serum-free medium was used as negative control (lanes 3 and 6). With an anti-GFP antibody, we detected apoER2 proteins as two bands (~120 and 145 kDa, top panel), which probably originate from differential glycosylation of the receptors (31). Sepp1 signal was detected only in lysates from cells transfected with apoER2-GFP and exposed to Sepp1^{+/+} serum (lane 8). The size of the detected band corresponded to that of the long isoform but not Sepp1 ^{Δ 240–361}. This observation was confirmed by the combination of Sepp1 ^{Δ 240–361} and apoER2-GFP or serum and GFP. Thus, we confirmed that Sepp1 ^{Δ 240–361} does not bind apoER2, in agreement with previous studies using immunostaining and ⁷⁵Se-Sepp1 uptake experiments (30). To characterize the Sepp1 and apoER2 binding, we conducted an ELISA-based solid phase binding assay using immunoaffinity-purified

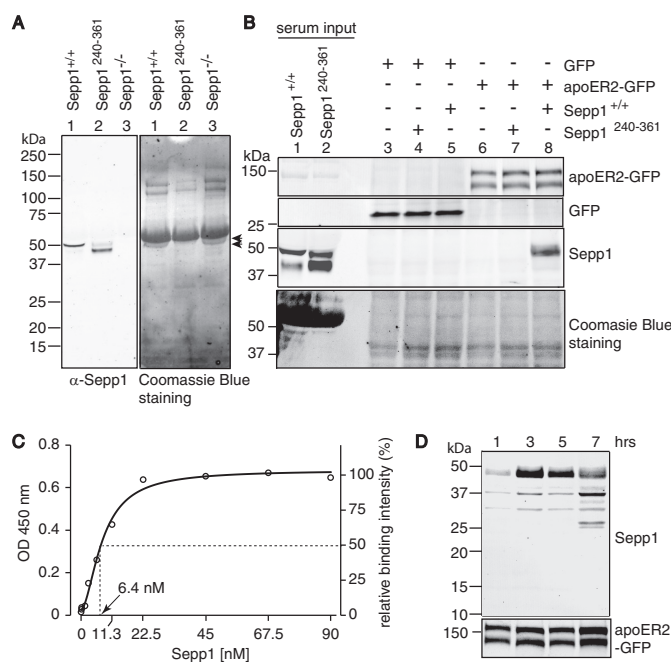


FIGURE 1. Sepp1 ^{Δ 240–361} does not bind to apoER2. A, left panel shows a Western blot of Sepp1 from Sepp1^{+/+} (lane 1), Sepp1 ^{Δ 240–361} (lane 2), or Sepp1^{-/-} (lane 3) mouse sera detected with anti-Sepp1 antibody. Right panel shows Coomassie Blue staining of the left panel membrane. Arrowheads show expected sizes of Sepp1 bands. No specific immunoreactive bands were detected in Sepp1^{-/-} serum (lane 3). B, the top two panels show Western blots of apoER2-GFP protein (top panel) or GFP protein (second panel) overexpressed in HEK293T cells detected with anti-GFP antibody. The third panel shows Sepp1 protein in sera from Sepp1^{+/+} or Sepp1 ^{Δ 240–361} mice and binding of Sepp1 protein to HEK293T cells, detected with anti-Sepp1 antibody. Coomassie Blue staining of the membrane is shown as protein loading control in the bottom panel. Molecular masses (kDa) are shown on the left. C, binding of Sepp1 to apoER2. 96-well plates were coated with 5 μ g/ml apoER2-GFP. After incubation with immunoaffinity-purified Sepp1 (0, 1.4, 2.8, 5.6, 11.3, 22.5, 45, 67.5, and 90 nM), bound Sepp1 was detected with rabbit anti-Sepp1 antibody and HRP-conjugated secondary antibody. D, Sepp1 internalization and degradation. Top panel, Western blot analysis of Sepp1 proteins. 10% mouse sera was incubated with apoER2-GFP-overexpressing HEK293T cells. After 1, 3, 5, and 7 h of incubation, cells were washed and lysed for Western blot analysis. ApoER2-GFP was used as protein loading control in the bottom panel.

Sepp1. Fig. 1C shows the binding of Sepp1 to apoER2 saturated at a concentration of 35 nM with a *K_d* of 6.4 nM. The affinity of Sepp1 for apoER2 was stronger than the reported value for RAP (13 nM) (32). Furthermore we characterized the time course for degradation of Sepp1 following apoER2 binding. After 3 h of incubation at 37 °C, we observed maximum binding of full-length Sepp1 to HEK293T cells expressing apoER2-GFP (Fig. 1D, 3 h lane). Further incubation resulted in smaller bands (25–37 kDa), suggesting cellular degradation of Sepp1. The half-time of ligand internalization of apoER2 (8 min) is much slower than that of very low density lipoprotein receptor (VLDLR) (30 s) (33), and overexpression of apoER2 further slows ligand internalization (34). We conducted the binding assay at 4 °C for 4 h to minimize endocytosis activity. The detected level of full-length Sepp1 observed was comparable with that following incubation at 37 °C for 3 h (data not shown). Thus, we found that 3 h of incubation of Sepp1 was adequate for detecting bound Sepp1 in this study. In the absence of cultured cells, we could not detect mouse Sepp1 degradation even after 3 days at 37 °C (data not shown).

Selenoprotein P and Apolipoprotein E Receptor-2 Interaction

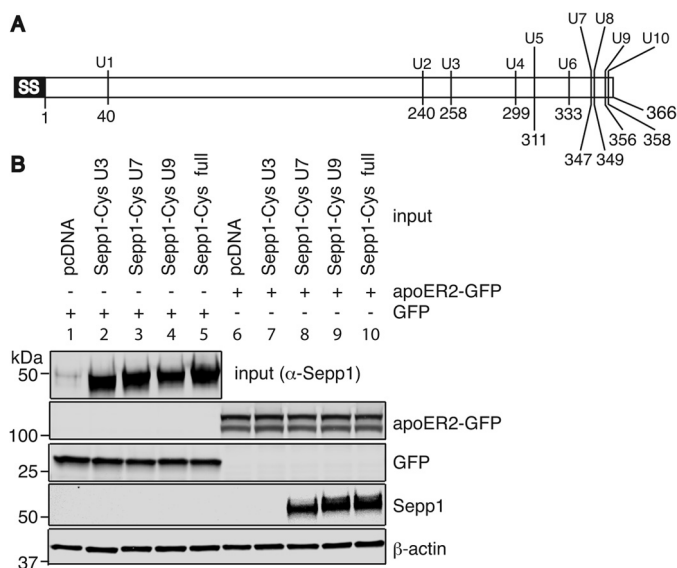


FIGURE 2. Longer Sepp1 isoforms bind to apoER2. *A*, schematic diagram of mouse Sepp1 showing location of selenocysteine residues. *B*, Sepp1 binding assay. TGA codons for selenocysteines were mutated to TGT (Se-Cys^{1–4} and Se-Cys^{7–10}) or TGC (Se-Cys⁵ and Se-Cys⁶), which encode cysteine. Sepp1-cys^{Δ258–361} (U3), Sepp1-cys^{Δ347–361} (U7), Sepp1-cys^{Δ356–361} (U9), and full-length Sepp1-cys (full) were constructed by site-directed mutagenesis. *Top panel*, HEK293T cells were transfected with Sepp1-cys constructs or pcDNA (lanes 1 and 6) as a negative control and Sepp1-cys mutants secreted into DMEM were detected by anti-Sepp1 antibody. Concentrated medium from these transfections were used as input in the binding assay. HEK293T cells were transiently transfected with a GFP construct (lanes 1–5) or the apoER2-GFP construct (lanes 6–10). ApoER2-GFP (*second panel*) or GFP (*third panel*) proteins were detected with anti-GFP antibody. Two days post-transfection, HEK293T cells were incubated with negative control (lanes 1 and 6), Se-Cys³ (lanes 2 and 7), Se-Cys⁷ (lanes 3 and 8), Se-Cys⁹ (lanes 4 and 9), or full-length (lanes 5 and 10) Sepp1-cys-containing media. Sepp1-cys mutants bound to HEK293T cells were detected with anti-Sepp1 antibody (*fourth panel*). Western blot analysis of β-actin was used as protein loading control in the *bottom panel*.

Because Sepp1^{+/+} contains several isoforms that are difficult to isolate, we produced mutant proteins terminating at the specific UGA codons by transient transfection in HEK293T cells. Fig. 2*A* shows location of selenocysteine residues. We introduced cysteine mutations in place of the selenocysteine residues of Sepp1 to avoid difficulties with overexpressing selenoproteins. We anticipated that mouse Sepp1 would produce four isoforms in plasma as found in rat Sepp1, because the Sepp1 protein sequences share 78% sequence homology. We expressed full-length mouse Sepp1-cys mutant proteins and Sepp1-cys mutants terminating at the third and seventh UGA, corresponding to isoforms previously identified in rat serum (11), as well as a mutant terminating at the ninth UGA. HEK293T cells successfully produced and secreted Sepp1-cys mutants into the culture media (Fig. 2*B*, lanes 2–5, *top panel*). Sepp1 was not detected in media from HEK293T cells transfected with empty vector (*lane 1*). HEK293T cells overexpressing GFP (lanes 1–5) or apoER2-GFP (lanes 6–10) proteins were incubated with media containing the different Sepp1-cys mutants, respectively. Full-length Sepp1-cys mutant was detected in lysates from cells transfected with the apoER2-GFP protein, indicating that the cysteine substitution for selenocysteine residues did not prevent Sepp1 binding (*lane 10*). Furthermore, Sepp1-cys mutants terminating at the seventh and ninth UGAs also bound to apoER2-GFP (lanes 8 and 9). Thus, apoER2 can

take up the longer Sepp1 isoforms containing six or more selenocysteine residues.

Essential Binding Sites for ApoER2 Are Located between Se-Cys³¹¹ and Se-Cys³³³ of Mouse Sepp1—We further narrowed down the potential binding site using Sepp1 constructs with a V5 epitope tag introduced between the signal sequence and N-terminal domain of Sepp1 using linker peptides (Fig. 3*A*). Fig. 3*B* shows that V5-Sepp1-cys proteins were successfully expressed by HEK293T cells and secreted into media (*top panel*). V5-Sepp1-cys mutants terminating at the fourth, fifth, or sixth UGA codons were added to GFP (lanes 1–3)- or apoER2-GFP (lanes 4–6)-overexpressing HEK293T cells. Only the mutants terminating at the sixth UGA bound to apoER2-GFP (*lane 6*), whereas mutants terminating at the fourth or fifth UGAs were undetected. Thus, the region between the fifth and sixth UGA codons of Sepp1 is necessary for apoER2 binding.

V5-Sepp1-cys mutants truncated at Ser³²⁴ and Pro³²⁹ (Δ324–361 and Δ329–361, respectively) were produced and used for the binding assay. Sepp1^{Δ329–361} but not Sepp1^{Δ324–361} bound to apoER2 (data not shown). Additionally, four other truncated mutants (Δ325–361, Δ326–361, Δ327–361, and Δ328–361) were produced, and apoER2 binding activity was assessed (Fig. 3*C*, *top panel*). Sepp1^{Δ328–361} was the shortest C-terminally truncated isoform that could bind to apoER2-GFP (*lane 5*).

CQC Residues of Sepp1 Are Essential for ApoER2 Binding—To verify that there were no additional domains within the truncated C-terminal domain (Sepp1^{328–361}) contributing to Sepp1 binding, full-length Sepp1 with sequential deletions between the Ser³²³ and Se-Cys³⁴⁹ residues were assayed (Fig. 4, *A* and *B*). Full-length V5-Sepp1-cys and V5-Sepp1-cys without Arg³²⁷ bound to apoER2 (Fig. 4*B*, *bottom panel*). Thus, Arg³²⁷ and the C-terminal domain between 328 and 361 likely do not contribute to Sepp1 binding activity. To identify essential binding residues, single alanine mutations were introduced into the full-length V5-Sepp1-cys. Fig. 4*D* shows that the mutants with alanine substitutions S323A and R327A were able to bind apoER2, but alanine substitutions C324A and C326A abolished apoER2 binding. The Q325A mutant also significantly reduced the binding activity. Fig. 4*D* shows the relative binding activity measured as the ratio of V5-Sepp1-cys to apoER2 immunoreactivity. Thus, residues Cys³²⁴, Gln³²⁵, and Cys³²⁶ (CQC) are likely to be essential binding residues of Sepp1.

Multiple Sequence Alignment Shows CQC Residues Are Highly Conserved in Sepp1—Fig. 5 shows the alignment of the C-terminal region of Sepp1 among various vertebrate animals. Interestingly, the CQC residues identified in this study are highly conserved. In some species, selenocysteine replaces one or both of the cysteine residues of the CQC sequence.

The N-terminal Domain of Sepp1 Is Not Required for ApoER2 Binding—Megalin, also known as Lrp2, is another member of the low density lipoprotein receptor family (35). Megalin is present on the brush border of renal proximal convoluted tubule cells and facilitates Sepp1 uptake. Megalin knock-out mice lose selenium through urine in the form of 11 N-terminal Sepp1 isoforms (22, 23). The fragments are truncated between the two histidine-rich (H-rich) regions, presumably by pro-

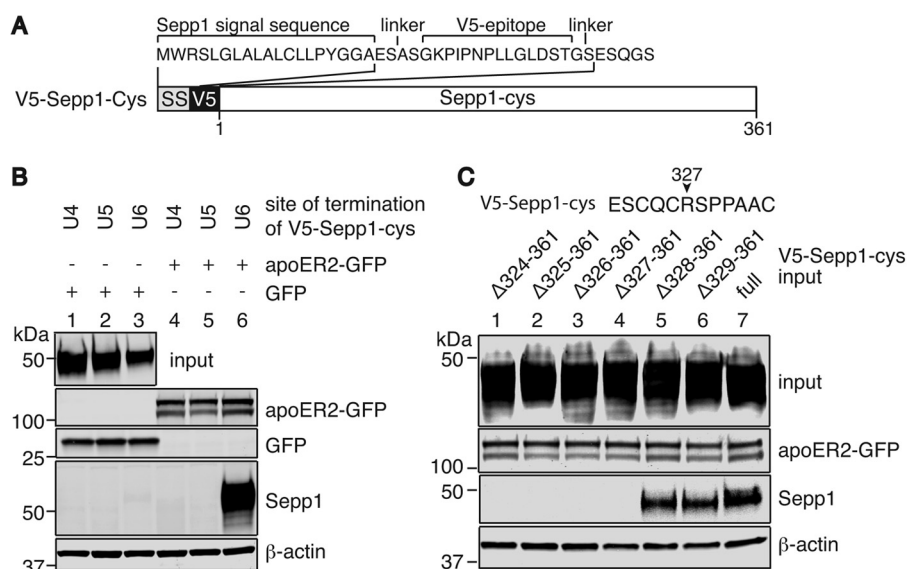


FIGURE 3. Essential binding sites for apoER2 are located between Se-Cys³¹¹ and Se-Cys³³³ of mouse Sepp1. *A*, schematic diagram of V5 tag in N terminus of Sepp1. V5 tag was inserted after the signal sequence of Sepp1 with linker peptides for easy detection by Western blot analyses. *B*, *top panel*, HEK293T cells were transfected with Sepp1-cys constructs, and Sepp1-cys mutants were secreted into DMEM and then were detected by anti-Sepp1 antibody. Concentrated media were used as input. HEK293T cells were transiently transfected with GFP construct (*lanes 1–3*) or apoER2-GFP construct (*lanes 4–6*), and 2 days later cells were incubated with Sepp1-cys^{Δ299–361} (U4-stop, *lanes 1 and 4*), Sepp1-cys^{Δ311–361} (U5-stop, *lanes 2 and 5*), or Sepp1-cys^{Δ333–361} (U6-stop, *lanes 3 and 6*)-containing media. ApoER2-GFP (*second panel*) or GFP (*third panel*) proteins were detected with anti-GFP antibody. Sepp1-cys mutants bound to HEK293T cells were detected with anti-Sepp1 antibody in the *fourth panel*. Western blot analysis of β-actin was used as protein loading control in the *bottom panel*. *C*, a partial Sepp1-cys sequence from Glu³²² to Cys³³³ is shown. *Top panel*, HEK293T cells were transfected with C-terminal deletion constructs (*lanes 1–6*) or full-length V5-Sepp1-cys constructs (*lane 7*) and V5-Sepp1-cys mutant proteins secreted into DMEM were detected by anti-V5 antibody. Concentrated media were used as an input. HEK293T cells were transiently transfected with apoER2-GFP construct, and 2 days later cells were incubated with Δ324–361 (*lane 1*), Δ325–361 (*lane 2*), Δ326–361 (*lane 3*), Δ327–361 (*lane 4*), Δ328–361 (*lane 5*), Δ329–361 (*lane 6*), or full-length (*lane 7*) V5-Sepp1-cys-containing media. ApoER2-GFP proteins were detected with anti-GFP antibody in the *second panel*. V5-Sepp1-cys mutants bound to HEK293T cells were detected with anti-V5 antibody in the *third panel*. Western blot analysis of β-actin was used as protein loading control in the *bottom panel*.

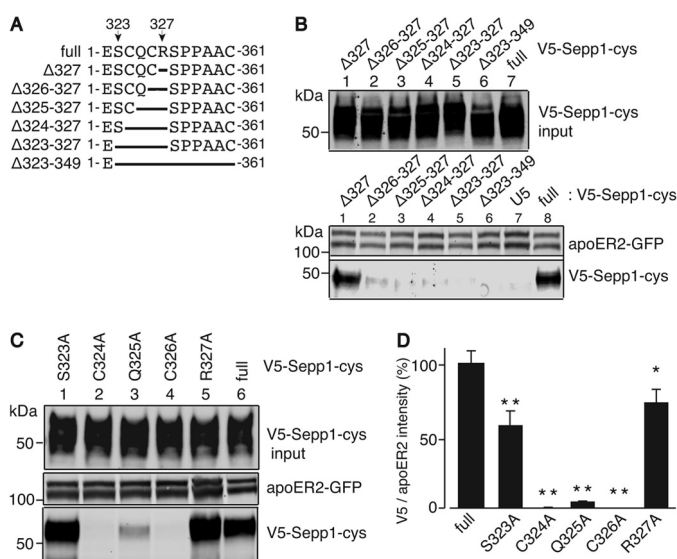


FIGURE 4. CQC residues of Sepp1 are essential for binding to apoER2. *A*, a diagram of deletion mutants used in this study. Sepp1-cys sequence from Glu³²² to Cys³³³ and deletion mutants in this region are shown. *B*, *top panel*, overexpressed V5-Sepp1-cys deletion mutants detected with anti-V5 antibody. HEK293T cell apoER2 protein detected with anti-apoER2 antibody (*second panel*); Western blot of V5-Sepp1-cys deletion mutants bound to apoER2, detected with anti-V5 antibody (*bottom panel*). *C*, *top panel*, overexpressed V5-Sepp1-cys alanine substitution mutants detected with anti-V5 antibody. HEK293T cell apoER2 protein detected with anti-apoER2 antibody (*second panel*); Western blot of V5-Sepp1-cys alanine substitution mutants bound to apoER2, detected with anti-V5 antibody (*bottom panel*). *D*, quantitation of V5-Sepp1-cys alanine substitution mutants bound to apoER2. The error bars represent standard error of the means ($n = 4$). *, $p < 0.05$; **, $p < 0.01$.

teases. The Sepp1 heparin-binding site is located in the N-terminal domain (residues 79–86) (Fig. 6A) (10), and heparin binding facilitates Sepp1 uptake in the rat L8 muscle cell line (30). It is speculated that heparin binding may facilitate access of proteases to the two H-rich stretches. In human plasma, proteases of the kallikrein family cleave Sepp1 into N-terminal and C-terminal fragments (8). We could not detect the C-terminal cleavage fragment of Sepp1 in megalin knock-out mice urine. Thus, there has been great interest in determining whether apoER2 could bind only the C-terminal domain. To assess the binding activity of the C-terminal domain, GFP was fused at the N terminus of full-length Sepp1 (GFP-Sepp1-cys) or constructs lacking amino acids 1–186 and 1–207 (designated as GFP-Sepp1 187–361 and GFP-Sepp1-cys 208–361, respectively) (Fig. 6B). ApoER2-GFP-expressing HEK cells were incubated with the GFP-Sepp1-cys protein isoforms. Fig. 6D shows that all of the constructs bind apoER2 (*lanes 4–6*). Thus, the heparin-binding site in the N-terminal domain of Sepp1 is not an essential domain for apoER2 binding. However, H-rich stretches as well as the heparin-binding site of Sepp1 may be capable of binding heparan sulfate proteoglycan because of their positive charges (10). To determine whether heparin alters the apoER2-binding ability of Sepp1 isoforms lacking most of the N-terminal region but containing the histidine-rich regions in addition to the C-terminal domain, we incubated Sepp1 isoforms with heparin prior to binding. Heparin did not inhibit the binding to apoER2 (Fig. 6E, *lanes 2, 4, and 6*). Thus, heparin binding activity of Sepp1 is not essential for apoER2 binding.

Selenoprotein P and Apolipoprotein E Receptor-2 Interaction

M. musculus	SUQGLFAEEK-VT ESCQCR -SPPAAUQ-NQPMNP-----MEANPNUSUDNQTRKUKUHSN	380
R. norvegicus	SCQGLFAEEK-VI ESCQCR -SPPAACH-SQHVSF-----TEASPNCSCNNKTKKCKCNLN	385
C. griseus	SUQGLFAEEK-VI ESCQCR -SPPAAUQ-SQPLDP-----TGASPNUSUDNKIKKUKURSN	383
J. jaculus	SUQGLFVAEK-VI ESCQUR -MPPAAUQ-SQQPKP-----TELSFN-UKUDKAKR-----	371
T. truncatus	SUQGLLAEEH-VT ESUQUR -LPPAACHATQQLKP-----TEASTKUSUKKAEMUKUPS	373
S. scrofa	SUQGLLAEEH-VI ESUQUR -LPPAAUQASQQLNP-----AEASTKUSUKNKAGRUKUPS	390
H. sapiens	SUQGLRAEEN-IT ESQUR -FPPAAUQISQQLIP-----TEASASURUKNOAKKUEUPS	381
O. cuniculus	SUQGLLAEEH-VI ESQUR -LPPAAUQTSQQLKP-----TEASTNUSUNNLAKKUKUPS	383
X. tropicalis	SUQELLSDS--L ESUQUR -LSAAAHSESTGLPETKLESEPNAPUAUPQEAENUQUKEL	397
G. gallus	RCHGQLLAED-IT ESQUR -LLTAACESAAGGGS-----ETSDFTCQCRERAGNCAKTN	393
D. rerio	PCQGLKEQDNH IKETCQCR PAPPAECELSPQTCVC-----PAGDATCGCRKK-----	367

: . : * : * * . * .
 : . : * : * * . * .

FIGURE 5. Multiple sequence alignment of partial C-terminal region of Sepp1 protein shows highly conserved CQC residues. The alignment was obtained with the program CLUSTAL W. Arrows indicate essential residues for apoER2 binding, identified in this study. Letters with black background residues indicate the identical amino acids in the alignment. Asterisks indicate positions that have a single, fully conserved residue, colons indicate conservation between groups of strongly similar properties, and periods indicate conservation between groups of weak similarity according to the Gonnet Pam 250 matrix by CLUSTAL W. The strong and weak groups are defined as a strong score of >0.5 and a weak score of ≤ 0.5 , respectively.

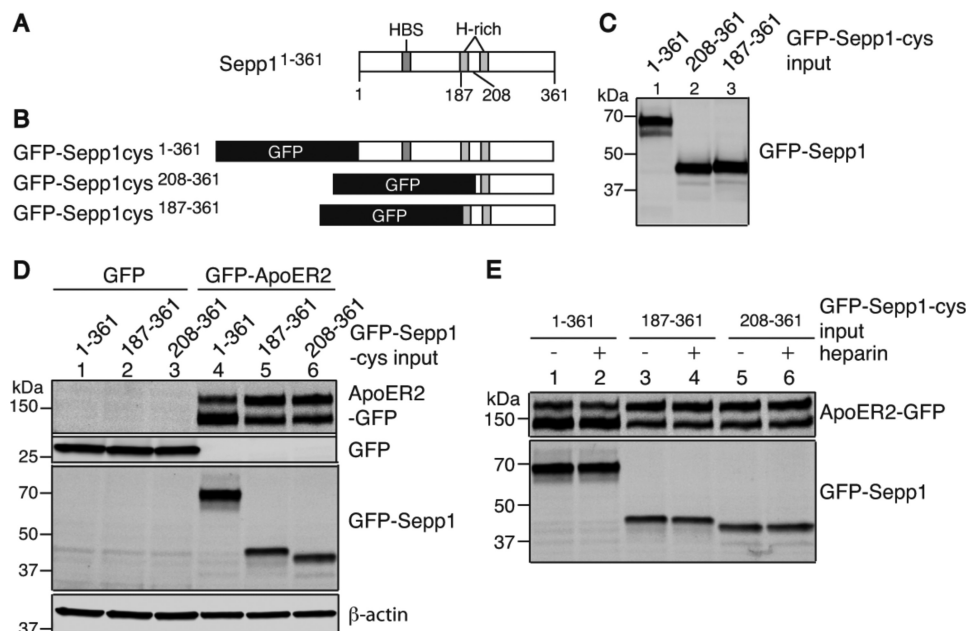


FIGURE 6. **Sepp1 N-terminal domain is not essential for binding to apoER2.** A, schematic diagram showing where Sepp1 is truncated in isoforms identified in megalin knock-out mouse urine. Sepp1 isoforms were truncated at residue 186 between a heparin-binding site and the two H-rich regions and at residue 207 between the H-rich regions. B, schematic diagram of GFP-Sepp1-cys constructs. GFP was fused to the N terminus of full-length Sepp1 protein (GFP-Sepp1-cys 1–361). For the missing region of Sepp1 proteins, N-terminal residues of Sepp1 (residues 1–186 or 1–207) were removed (GFP-Sepp1-cys 187–361 and GFP-Sepp1-cys 208–361, respectively). C, HEK293T cells were transfected with GFP-Sepp1-cys constructs, and GFP-Sepp1-cys mutants were detected by anti-GFP antibody. GFP-Sepp1 proteins were detected as proteins with expected sizes of 68 kDa (lane 1, GFP-Sepp1-cys 1–361), 40 kDa (lane 2, GFP-Sepp1-cys 208–361), and 42 kDa (lane 3, GFP-Sepp1-cys 187–361). D, upper two panels, GFP proteins (lanes 1–3) and apoER2-GFP proteins (lanes 4–6) were detected with anti-GFP antibody. Third panel, GFP-Sepp1-cys mutants bound to HEK293T cells were detected with anti-GFP antibody. GFP-Sepp1-cys 1–361 (lanes 1 and 4), GFP-Sepp1-cys 187–361 (lanes 2 and 5), or GFP-Sepp1-cys 208–361 (lanes 3 and 6) was incubated with HEK293T cells overexpressing GFP protein (lanes 1–3) and apoER2-GFP protein (lanes 4–6). Western blot analysis of β -actin was used as protein loading control (bottom panel). E, top panel, GFP-apoER2 proteins were detected with anti-GFP antibody. Bottom panel, GFP-Sepp1-cys 1–361 (lanes 1 and 2), GFP-Sepp1-cys 187–361 (lanes 3 and 4), and GFP-Sepp1-cys 208–361 (lanes 5 and 6) were incubated with HEK293T cells in the presence of heparin (2.5 mg/ml) (lanes 2, 4, and 6) or not (lanes 1, 3, and 5). GFP-Sepp1-cys proteins were detected with anti-GFP antibody.

RAP Protein Does Not Interfere with Sepp1 Binding to ApoER2—Other ligands of apoER2 (e.g., apoE, reelin, and thrombospondin) bind to the extracellular LBRs of apoER2. The low density lipoprotein receptor-associated protein (RAP) is a well characterized protein, which functions as a chaperone protein in the endoplasmic reticulum (36). RAP binds to the LBRs of low density lipoprotein receptor with a K_d of 5.64 nM (37) to prevent receptor aggregation and degradation. RAP interferes with the binding of Sepp1 to megalin (16), suggesting that Sepp1 likely binds to the LBRs of megalin. To see whether Sepp1 binds to the LBRs of apoER2, we determined whether

RAP protein interfered with Sepp1-apoER2 binding. We purified RAP with a six-histidine tag (RAP-His) and incubated it prior to the Sepp1 binding assay. Figs. 7 shows that RAP protein does not compete with Sepp1. RAP has been reported to copurify with apoER2 on a Sepp1-immobilized column from testis membrane fraction (6). This indicates Sepp1 occupies a different binding site of apoER2 where it does not interfere with RAP protein binding.

Sepp1 Binds to the β -Propeller Domain of ApoER2—The extracellular region of mouse apoER2 consists of four types of protein domains. These include the LBR, the EGF repeat, the

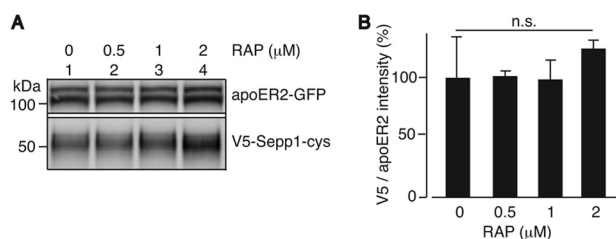


FIGURE 7. RAP protein does not compete with Sepp1 binding to apoER2. A, Sepp1 protein and indicated concentrations of purified RAP protein were incubated with HEK293T cells expressing apoER2-GFP. Shown is a Western blot of the apoER2-GFP protein overexpressed in HEK293T cells detected with anti-GFP antibody (*top panel*) and Sepp1 protein detected with anti-Sepp1 antibody (*bottom panel*). B, relative Sepp1 binding to apoER2 in the presence of RAP protein was quantified. Error bars represent standard error of the means ($n = 3$).

YWTD β -propeller domain, and the O-linked sugar domain. To determine the apoER2 domain that binds Sepp1, mutants with sequential extracellular domain deletions of apoER2-GFP were produced (Fig. 8A). HEK293T cells express undetectable amounts of native apoER2 (Fig. 8B, *left panel, lane 1*), and overexpressed apoER2-GFP protein could be detected with an anti-apoER2 antibody (*lane 2*). The GFP and apoER2-GFP mutant proteins were overexpressed in HEK293T cells (Fig. 8C, *top panel, lanes 2–9*). Because the signal sequence and transmembrane domain were intact for each mutant, GFP could be observed on the plasma membrane with fluorescent microscopy (data not shown). This indicated that the mutant proteins were localized to the cell surface. HEK293T cells expressing the mutant apoER2-GFP constructs were incubated in mouse Sepp1^{+/+} serum. Fig. 8C (*second panel*) shows that full-length apoER2, apoER2 without LBRs, and apoER2 without LBR and EGF repeats can bind Sepp1 (*lanes 3–5*, respectively). Interestingly, apoER2-GFP mutants without the YWTD β -propeller domain lost Sepp1 binding activity (*lanes 6–9*). The experiment using the apoER2-GFP mutant lacking the YWTD β -propeller domain but not the ligand binding repeats clearly demonstrates that Sepp1 does not bind when the β -propeller is missing (*lane 9*).

An ApoER2 Variant Located in Placenta That Has a Furin Cleavage Site Is Expressed as Full-length ApoER2—ApoER2 has several splice variants (38), one of which includes a 13-amino acid furin consensus cleavage site between the LBRs and EGF repeat A domain (31). This cleavable apoER2 variant has been suggested to play a different function in brain after the soluble extracellular domain of apoER2 is cleaved by furin in the endoplasmic reticulum (32). The 23-kDa soluble receptor fragment is then secreted from cells to bind reelin and thus functions in a dominant-negative fashion in the regulation of reelin signaling during embryonic brain development (32). The remaining membrane-spanning part of apoER2-containing repeat A of the EGF precursor homology domain might be degraded rapidly under these conditions.

However, the mRNA of the furin-cleavable form of apoER2 is the only detectable variant in placenta and is highly expressed in this tissue (Fig. 9A, *row b*) (31). Because Sepp1 has been shown to be taken up by apoER2 in placenta (21), we investigated the form of apoER2 in this tissue. Testis also has very high expression of apoER2, and expresses mRNA for both the cleav-

able and noncleavable forms (Fig. 9A, *rows a and b*) (6). From this study, it is expected that RAP and Sepp1 bind and pull down different domains of apoER2. Membrane fractions of adult testis or placenta from adult female at gestational day 15 were collected, purified by Sepp1 or RAP-immobilized resin, and applied to SDS-PAGE. ApoER2 was detected by Western blot using anti-apoER2 antibody recognizing the C-terminal domain of apoER2. Fig. 9B shows both Sepp1 and RAP-immobilized resins are capable of binding apoER2. Because the apoER2 signals eluted from Sepp1 and RAP-immobilized resins show the same migration pattern on the SDS-PAGE, placenta apoER2 contains the LBR. The testis apoER2 signal also suggests that the furin cleavage site of apoER2 in the tissue is not cleaved.

Sepp1 Endocytosis and Utilization Does Not Require the LBR of ApoER2—Dissociation of ligands is crucial for receptor recycling and proper receptor function (39). The LDL receptor-recycling pathway has been well characterized (40). Receptors bind their ligands via the LBRs at neutral extracellular pH. The receptor and its ligand are then internalized in clathrin-coated vesicles.

Endocytosis of Sepp1 takes place by a clathrin-dependent mechanism (30). Once the clathrin-coated vesicle uncoats and fuses to form the early endosome, ligands can be released from LBRs by acidification of the endosome, generated by a vacuolar membrane proton pump V-ATPase. At acidic pH (<6.0) in the endosomes, the YWTD β -propeller domain may undergo a conformational change, occupying the LBRs and displacing bound ligands. Thus, we examined whether apoER2-GFP mutants function in Sepp1 utilization through facilitating expression of the selenoprotein Gpx. Gpx1 is a major cytoplasmic selenoprotein, and selenium availability dramatically changes its protein expression (41). HEK293T cells overexpressing full-length apoER2-GFP, apoER2-GFP without the LBRs (Δ LBR), apoER2-GFP without the β -propeller domain (Δ BP), or GFP as a negative control were preincubated with serum-free medium for 48 h. Then medium was changed to medium with a lower level of mouse serum (0.2%) to minimize selenium uptake in non-apoER2 transfected cells. Cultures were incubated for 24 h. Cell lysates were analyzed with SDS-PAGE, and Gpx1 protein was detected by Western blot using anti-Gpx1 antibody. Fig. 9C shows that Gpx1 protein increased in lysates from cells expressing full-length apoER2-GFP and Δ LBR, but not in cells expressing Δ BP, or GFP alone. Fig. 9D shows the relative quantification of Gpx1 protein to β -actin protein. HEK293T cells overexpressing Δ LBR showed statistically significant expression of Gpx1 protein compared with GFP expressing cells. Although apoER2-GFP expressing cells do not show statistically significant changes, there is a similar increasing trend in Gpx1 protein expression. Thus, apoER2 facilitates Sepp1 uptake through its β -propeller domain to supply selenium for synthesis of Gpx1.

DISCUSSION

The results presented here demonstrate that the two longer isoforms of Sepp1 bind to apoER2, whereas shorter isoforms do not. Thus, only Sepp1 containing six or more selenocysteines can be taken up via apoER2, ensuring adequate uptake of sele-

Selenoprotein P and Apolipoprotein E Receptor-2 Interaction

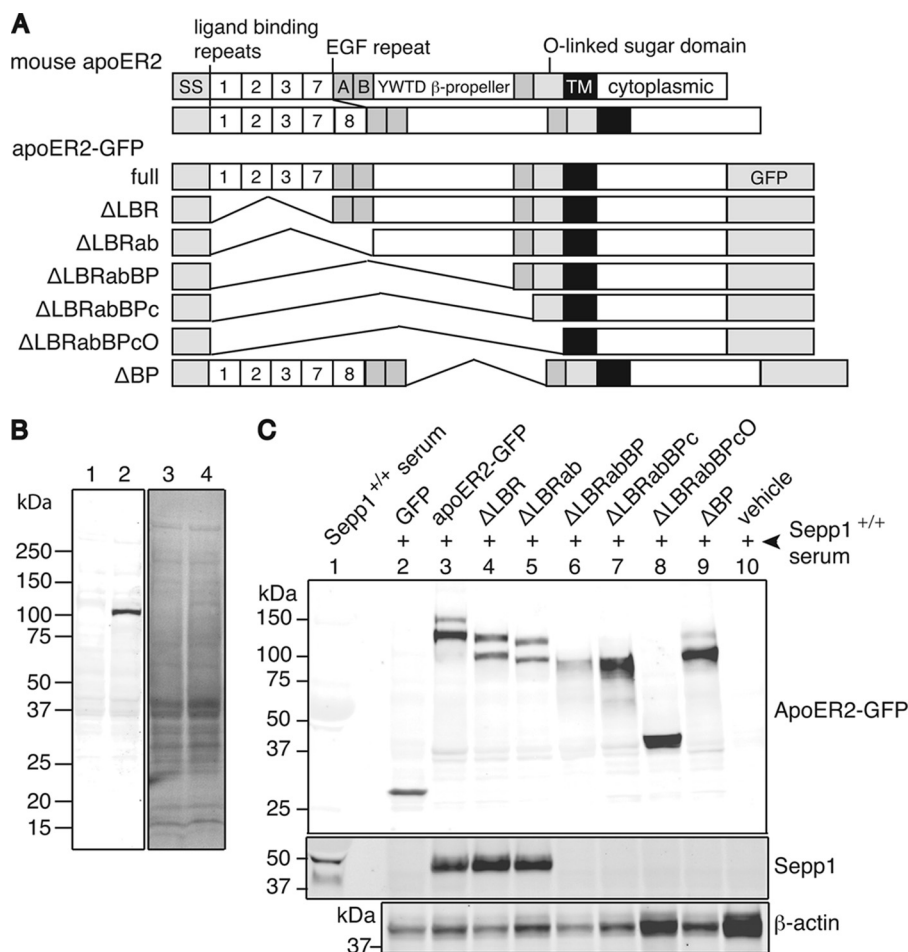


FIGURE 8. Sepp1 binds to the YWTD β -propeller domain of apoER2. *A*, schematic diagram of the native mouse apoER2 receptor and deletion variants used in Sepp1 binding assay. SS, signal sequence; 1, 2, 3, 7, and 8, ligand binding repeats; letters A, B, and C, cysteine-rich repeats in EGF precursor homology domain; TM, transmembrane domain. Mouse apoER2 has two different splice variants differing in one of the LBRs (LBR1237 or LBR12378). GFP was fused to the C terminus of full-length apoER2 (apoER2-GFP). ApoER2-GFP with LBR deletion (Δ LBR); LBR and EGF-AB deletion (Δ LBRab); LBR, EGF-AB, and YWTD β -propeller deletion (Δ LBRabBP); LBR, EGF-AB, YWTD β -propeller, and EGF-C deletion (Δ LBRabBPc); LBR, EGF-AB, YWTD β -propeller, EGF-C, and O-linked sugar domain deletion (Δ LBRabBPcO); LBR, EGF-AB, YWTD β -propeller, EGF-C, and O-linked sugar domain deletion (Δ BP) are shown. *B*, left panel shows a Western blot of the HEK293T cell apoER2 detected with anti-apoER2 antibody. Lane 1, whole cell lysate of pEGFP-C1 transfected HEK293T cells; lane 2, apoER2-GFP transfected HEK293T cells. Right panel shows Coomassie Blue staining of the membrane. *C*, lane 1 shows Sepp1^{+/+} serum used as input protein in Sepp1 binding assay. Top panel shows a Western blot of the apoER2-GFP mutant proteins (lanes 2–9) overexpressed in HEK293T cells detected with anti-GFP antibody. Lane 10 shows a vehicle control. Second panel shows a Western blot of the Sepp1 proteins bound to HEK293T cells overexpressing apoER2-GFP mutant proteins, detected with anti-Sepp1 antibody. Bottom panel shows a Western blot of β -actin protein detected with anti- β -actin antibody as protein loading control.

nium for selenoprotein synthesis. Further analysis showed that the N-terminal domain of Sepp1 is not essential and that the C-terminal domain is sufficient for apoER2 binding. Sepp1 binds to the β -propeller domain of apoER2, and uptake of selenium does not require the LBRs of apoER2. In contrast, all other known apoER2 ligands bind via the LBRs, making Sepp1 unique among known ligands in its binding to apoER2. An apoER2 variant occurs in placenta as full-length apoER2, although it has a furin cleavage site. These findings have implications for the selective uptake of Sepp1 by apoER2 and explain the Sepp1 isoform specificity of apoER2 *versus* megalin.

The *in vitro* binding assay established here confirmed that endocytosis of Sepp1 ^{Δ 240–361} does not occur via apoER2. Our findings imply that apoER2-mediated uptake of Sepp1 from plasma brings a minimum of six selenium atoms for each Sepp1 protein, ensuring efficient delivery to tissue requiring high sele-

nium intake. Neither the shortest isoform of Sepp1 nor Sepp1 truncated at the site of the third UGA are capable of binding apoER2 (Figs. 1 and 2), suggesting that these isoforms do not function in apoER2-mediated selenium delivery to tissues. The N-terminal domain of Sepp1 may function as a redox enzyme through its UXXC thioredoxin fold (42). A recent report showed that Sepp1 protects mice against *Trypanosoma congolense* infection, and Sepp1 ^{Δ 240–361} is sufficient for this function (43). This suggests the Sepp1 ^{Δ 240–361} isoform has alternative functions *in vivo*; thus, the isoform truncated at the third UGA may also have alternate functions. We also investigated the affinity of Sepp1 to apoER2. The plasma Sepp1 concentration of mice fed a diet of 0.25 ppm selenite was 18.5 μ g/ml, or 455 nM when estimating for full-length Sepp1. We estimated that Sepp1 has a relatively high affinity of K_d of 6.4 nM for apoER2. Based on the results presented in Fig. 1D, Sepp1 bound to

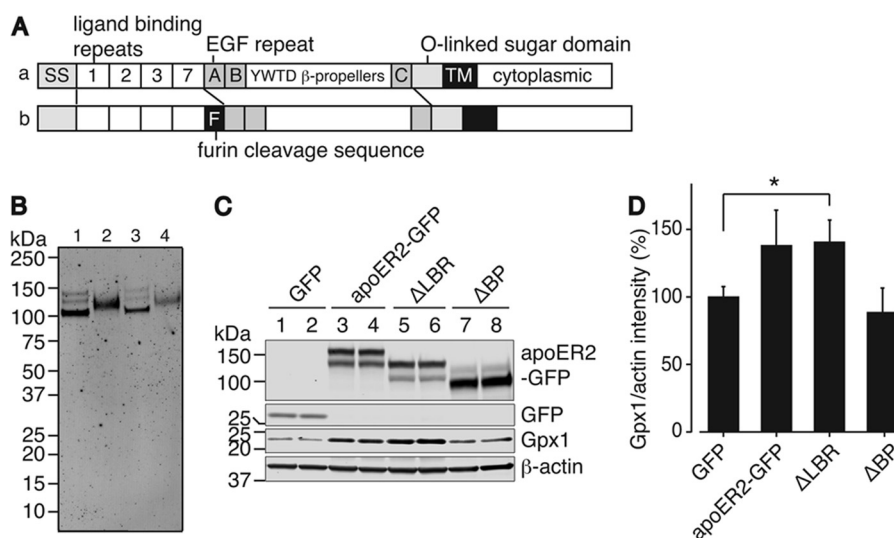


FIGURE 9. Placental apoER2 isoform and utilization of selenium derived from Sepp1 by apoER2 variants. *A*, diagrams comparing the domain structure of testis and placenta apoER2. One of two testis variants and a placental variant (row *b*) differ from the major isoform (row *a*) by the presence of a furin cleavage sequence. *SS*, signal sequence; 1, 2, 3, and 7, ligand binding repeats; letters *A*, *B*, and *C*, EGF repeat *A*, *B*, and *C*; *TM*, transmembrane domain. *B*, Western blot of the adult testis (lanes 1 and 3) and day 15 placenta (lanes 2 and 4) apoER2 protein stained with anti-apoER2 C-terminal peptide antibody. Lanes 1 and 2 show proteins bound to Sepp1 resin, and lanes 3 and 4 show proteins bound to RAP resin. *C*, top two panels show Western blot of GFP (lanes 1 and 2), full-length apoER2-GFP (lanes 3 and 4), apoER2-GFP LBR deletion (Δ LBR, lanes 5 and 6), or apoER2-GFP YWTD β -propeller deletion (Δ BP, lanes 7 and 8) proteins overexpressed in HEK293T cells and detected with anti-GFP antibody. The third panel shows Western blot of Gpx1 protein produced in HEK293T cells following expression of apoER2-GFP variants. Gpx1 protein was detected with anti-Gpx1 antibody. The bottom panel shows Western blot of β -actin protein detected with anti- β -actin antibody as protein loading control. *D*, relative Gpx1 protein to β -actin protein was quantified. Error bars represent standard error of the means ($n = 3$). The asterisk indicates that Δ LBR is different ($p < 0.05$) from GFP by Student's *t* test.

apoER2 is slowly broken down to lower migrating protein bands as the incubation time increases, suggesting that Sepp1 is being metabolized for recovery of selenium.

We narrowed down potential binding residues of Sepp1 for apoER2 binding via point mutations to show that the CQC (Cys³²⁴, Gln³²⁵, and Cys³²⁶) residues are required for binding. Although each CQC single-residue mutation diminishes or eliminates Sepp1 binding activity, these residues may be required for proper Sepp1 protein folding to facilitate binding. Short peptides of Sepp1 including the CQC stretch (H₂N-GL-FAEEKVTESCQCRS-OH) do not inhibit Sepp1 binding to apoER2, suggesting that proper conformation may be required for Sepp1 binding (data not shown). Two cysteine/selenocysteine residues can form disulfide/selenenylsulfide bonds. Previous studies of rat Sepp1 have not identified such bonding within the CQC residues (44), but there is a possibility that these residues can form disulfide bonds. ApoER2 bound to immobilized Sepp1-resin can be discharged by acidic conditions (6). This suggests the interaction is due either to salt bridge formation or ionic bonding. This observation also argues against direct disulfide bonds between Sepp1 and apoER2, because acidic conditions would not break disulfide bonds between the proteins. Thus, the actual mechanism of binding might be: 1) binding to a site containing the three residues or 2) binding to a site that depended on the three residues interacting with some other part of Sepp1, perhaps by disulfide or selenenylsulfide formation. Further structural studies are needed to clarify the Sepp1-apoER2 interaction.

Based on sequence alignment, the CQC residues are highly conserved among species. Some species have selenocysteine residues in place of cysteine residues within this sequence. Selenocysteine and cysteine residues share similar chemical char-

acteristics; thus, the mutation of cysteine to selenocysteine may still conserve Sepp1 binding activity. The conservation of the residues across a broad range of species suggests that this region is likely crucial for Sepp1 binding activity.

Sepp1 has a heparin-binding site in the N-terminal domain (10). Sepp1 heparin binding is pH-dependent (45) and is important for uptake by rat L8 cells (30). The heparin binding ability of Sepp1 has been proposed to increase the probability of binding to Sepp1 receptors via the cellular surface heparan sulfate proteoglycan. The H-rich domain has also been proposed as a potential heparin-binding domain (10). Recently, shorter Sepp1 fragments were found in the glomerular filtrate of the megalin knock-out mouse model (23). Mass spectrometry identified N-terminal fragments of Sepp1 from the urine. These fragments were missing one or both of the H-rich stretches. Although the mechanism of generation of such fragments needs further study, the fragments are likely generated by proteases. The C-terminal domain of Sepp1 (residues 208–361) binds to apoER2, whereas the N-terminal domain (residues 1–207) is not required. Unexpectedly, incubation with heparin does not interfere with Sepp1 binding to apoER2. It is possible that heparin binding can facilitate Sepp1 uptake kinetics for low Sepp1 receptor-expressing tissues such as muscle cells. In the present study, because of overexpression of apoER2 on the cellular surface, it is likely that Sepp1 binding does not require heparin binding activity.

ApoER2 interacts with a number of its specific ligand proteins through the extracellular domain. ApoER2 has four to five LBR domains. Reelin binds to the first LBR, and apoE binds to third LBR (26, 27). The RAP chaperone protein also binds to the third LBR (37), and both reelin and apoE compete with RAP for binding. In our binding studies, we did not observe any inter-

Selenoprotein P and Apolipoprotein E Receptor-2 Interaction

ference of RAP with Sepp1 binding, suggesting that Sepp1 does not compete for the same binding site. This is in agreement with our subsequent studies indicating that Sepp1 binds to the β -propeller domain instead of an LBR domain.

ApoER2 changes configuration in low pH conditions, allowing the β -propeller domain to bind directly to LBRs in competition with LBR ligands. This causes the release of ligands in endosomes at pH < 6. Selenium supply through apoER2-mediated endocytosis of Sepp1 presumably requires endosomal degradation for production of L-selenocysteine from Sepp1. Based on our results, synthesis of the selenoprotein Gpx1 is facilitated by overexpression of apoER2 mutants containing the β -propeller domain even in the absence of the LBR (Fig. 8). This suggests that Sepp1 uptake mechanism is different from LBR-binding ligands.

ApoER2 also facilitates reelin signaling, which is important for brain development and synaptic plasticity (46). Several transcripts of apoER2 are expressed as splice variants in different stages of development and in a tissue-specific manner. Some variants in brain and all variants in placenta have an exon encoding a 13-amino acid stretch containing a furin cleavage site (31). Cleavage by furin in brain produces a secreted soluble isoform that functions as a dominant negative receptor to regulate reelin signaling during embryonic brain development (32). Thus, splicing of the region encoding the extracellular domain of apoER2 has been suggested for the fine-tuning of ligand specificities. We found that placenta expresses a full-length apoER2, which indicates the furin cleavage does not occur during late gestation (day 15). Sepp1 is taken up in placenta by apoER2, as demonstrated by immunocytochemistry and measuring selenium (21). The furin cleavage site may thus have a different function in this tissue. However, the furin-cleaved apoER2 product may function as a specific receptor for Sepp1. ApoER2 endocytosis and degradation is induced by multivalent ligands and is facilitated by the lysosomal pathway (47). Further study is needed to determine whether Sepp1 induces endocytosis and proteolysis of apoER2.

In conclusion, the findings that apoER2 binds specific isoforms of Sepp1 in the C-terminal selenocysteine-rich domain and that they bind to the β -propeller domain of apoER2 suggest that Sepp1 uptake by apoER2-mediated endocytosis is highly efficient for selenium gathering and, further, that the mechanism of Sepp1 uptake is distinct from the LBR domain-mediated uptake of other ligands.

Acknowledgments—We thank Ali Seyedali and Christy Gilman for critical reading of the manuscript. We thank Ann Hashimoto for animal husbandry.

REFERENCES

1. Kryukov, G. V., Castellano, S., Novoselov, S. V., Lobanov, A. V., Zehtab, O., Guigó, R., and Gladyshev, V. N. (2003) Characterization of mammalian selenoproteomes. *Science* **300**, 1439–1443
2. Berry, M. J., Banu, L., Chen, Y. Y., Mandel, S. J., Kieffer, J. D., Harney, J. W., and Larsen, P. R. (1991) Recognition of UGA as a selenocysteine codon in type I deiodinase requires sequences in the 3' untranslated region. *Nature* **353**, 273–276
3. Mehta, A., Rebsch, C. M., Kinzy, S. A., Fletcher, J. E., and Copeland, P. R. (2004) Efficiency of mammalian selenocysteine incorporation. *J. Biol. Chem.* **279**, 37852–37859
4. Winkler, K., Böcher, M., Flohé, L., Kollmus, H., and Brigelius-Flohé, R. (1999) mRNA stability and selenocysteine insertion sequence efficiency rank gastrointestinal glutathione peroxidase high in the hierarchy of selenoproteins. *Eur. J. Biochem.* **259**, 149–157
5. Hill, K. E., Xia, Y., Akesson, B., Boeglin, M. E., and Burk, R. F. (1996) Selenoprotein P concentration in plasma is an index of selenium status in selenium-deficient and selenium-supplemented Chinese subjects. *J. Nutr.* **126**, 138–145
6. Olson, G. E., Winfrey, V. P., Nagdas, S. K., Hill, K. E., and Burk, R. F. (2007) Apolipoprotein E receptor-2 (apoER2) mediates selenium uptake from selenoprotein P by the mouse testis. *J. Biol. Chem.* **282**, 12290–12297
7. Hill, K. E., Wu, S., Motley, A. K., Stevenson, T. D., Winfrey, V. P., Capecci, M. R., Atkins, J. F., and Burk, R. F. (2012) Production of selenoprotein P (Sepp1) by hepatocytes is central to selenium homeostasis. *J. Biol. Chem.* **287**, 40414–40424
8. Saito, Y., Sato, N., Hirashima, M., Takebe, G., Nagasawa, S., and Takahashi, K. (2004) Domain structure of bi-functional selenoprotein P. *Biochem. J.* **381**, 841–846
9. Hill, K. E., Zhou, J., Austin, L. M., Motley, A. K., Ham, A. J., Olson, G. E., Atkins, J. F., Gesteland, R. F., and Burk, R. F. (2007) The selenium-rich C-terminal domain of mouse selenoprotein P is necessary for the supply of selenium to brain and testis but not for the maintenance of whole body selenium. *J. Biol. Chem.* **282**, 10972–10980
10. Hondal, R. J., Ma, S., Caprioli, R. M., Hill, K. E., and Burk, R. F. (2001) Heparin-binding histidine and lysine residues of rat selenoprotein P. *J. Biol. Chem.* **276**, 15823–15831
11. Ma, S., Hill, K. E., Caprioli, R. M., and Burk, R. F. (2002) Mass spectrometric characterization of full-length rat selenoprotein P and three isoforms shortened at the C terminus: evidence that three UGA codons in the mRNA open reading frame have alternative functions of specifying selenocysteine insertion or translation termination. *J. Biol. Chem.* **277**, 12749–12754
12. Berry, M. J., Banu, L., Harney, J. W., and Larsen, P. R. (1993) Functional characterization of the eukaryotic SECIS elements which direct selenocysteine insertion at UGA codons. *EMBO J.* **12**, 3315–3322
13. Stoytcheva, Z., Tujebajeva, R. M., Harney, J. W., and Berry, M. J. (2006) Efficient incorporation of multiple selenocysteines involves an inefficient decoding step serving as a potential translational checkpoint and ribosome bottleneck. *Mol. Cell. Biol.* **26**, 9177–9184
14. Schomburg, L., Schweizer, U., Holtmann, B., Flohé, L., Sendtner, M., and Köhrle, J. (2003) Gene disruption discloses role of selenoprotein P in selenium delivery to target tissues. *Biochem. J.* **370**, 397–402
15. Hill, K. E., Zhou, J., McMahan, W. J., Motley, A. K., Atkins, J. F., Gesteland, R. F., and Burk, R. F. (2003) Deletion of selenoprotein P alters distribution of selenium in the mouse. *J. Biol. Chem.* **278**, 13640–13646
16. Olson, G. E., Winfrey, V. P., Hill, K. E., and Burk, R. F. (2008) Megalin mediates selenoprotein P uptake by kidney proximal tubule epithelial cells. *J. Biol. Chem.* **283**, 6854–6860
17. Andersen, O. M., Yeung, C. H., Vorum, H., Wellner, M., Andreassen, T. K., Erdmann, B., Mueller, E. C., Herz, J., Otto, A., Cooper, T. G., and Willnow, T. E. (2003) Essential role of the apolipoprotein E receptor-2 in sperm development. *J. Biol. Chem.* **278**, 23989–23995
18. Ursini, F., Heim, S., Kiess, M., Maiorino, M., Roveri, A., Wissing, J., and Flohé, L. (1999) Dual function of the selenoprotein PhgpX during sperm maturation. *Science* **285**, 1393–1396
19. Olson, G. E., Winfrey, V. P., Nagdas, S. K., Hill, K. E., and Burk, R. F. (2005) Selenoprotein P is required for mouse sperm development. *Biol. Reprod.* **73**, 201–211
20. Kim, D. H., Iijima, H., Goto, K., Sakai, J., Ishii, H., Kim, H. J., Suzuki, H., Kondo, H., Saeki, S., and Yamamoto, T. (1996) Human apolipoprotein E receptor 2: a novel lipoprotein receptor of the low density lipoprotein receptor family predominantly expressed in brain. *J. Biol. Chem.* **271**, 8373–8380
21. Burk, R. F., Olson, G. E., Hill, K. E., Winfrey, V. P., Motley, A. K., and Kurokawa, S. (2013) Maternal-fetal transfer of selenium in the mouse. *FASEB J.* **27**, 3249–3256

22. Kurokawa, S., Eriksson, S., Rose, K. L., Wu, S., Motley, A. K., Hill, S., Winfrey, V. P., McDonald, W. H., Capecchi, M. R., Atkins, J. F., Arner, E. S., Hill, K. E., and Burk, R. F. (2014) Sepp1^{UF} forms are N-terminal selenoprotein P truncations that have peroxidase activity when coupled with thioredoxin reductase-1. *Free Radic. Biol. Med.* **69C**, 67–76
23. Chiu-Ugalde, J., Theilig, F., Behrends, T., Drebes, J., Sieland, C., Subbarayal, P., Köhrle, J., Hammes, A., Schomburg, L., and Schweizer, U. (2010) Mutation of megalin leads to urinary loss of selenoprotein P and selenium deficiency in serum, liver, kidneys and brain. *Biochem. J.* **431**, 103–111
24. May, P., Herz, J., and Bock, H. H. (2005) Molecular mechanisms of lipoprotein receptor signalling. *Cell. Mol. Life. Sci.* **62**, 2325–2338
25. Masiulis, I., Quill, T. A., Burk, R. F., and Herz, J. (2009) Differential functions of the apoER2 intracellular domain in selenium uptake and cell signaling. *Biol. Chem.* **390**, 67–73
26. Hibi, T., Mizutani, M., Baba, A., and Hattori, M. (2009) Splicing variations in the ligand-binding domain of apoER2 results in functional differences in the binding properties to reelin. *Neurosci. Res.* **63**, 251–258
27. Yamagata, M., Ozono, K., Hashimoto, Y., Miyauchi, Y., Kondou, H., and Michigami, T. (2005) Intraperitoneal administration of recombinant receptor-associated protein causes phosphaturia via an alteration in subcellular distribution of the renal sodium phosphate co-transporter. *J. Am. Soc. Nephrol.* **16**, 2338–2345
28. Seale, L. A., Hashimoto, A. C., Kurokawa, S., Gilman, C. L., Seyedali, A., Bellingier, F. P., Raman, A. V., and Berry, M. J. (2012) Disruption of the selenocysteine lyase-mediated selenium recycling pathway leads to metabolic syndrome in mice. *Mol. Cell. Biol.* **32**, 4141–4154
29. Hill, K. E., Zhou, J., McMahan, W. J., Motley, A. K., and Burk, R. F. (2004) Neurological dysfunction occurs in mice with targeted deletion of the selenoprotein P gene. *J. Nutr.* **134**, 157–161
30. Kurokawa, S., Hill, K. E., McDonald, W. H., and Burk, R. F. (2012) Long isoform mouse selenoprotein P (Sepp1) supplies rat myoblast L8 cells with selenium via endocytosis mediated by heparin binding properties and apolipoprotein E receptor-2 (apoER2). *J. Biol. Chem.* **287**, 28717–28726
31. Brandes, C., Kahr, L., Stockinger, W., Hiesberger, T., Schneider, W. J., and Nimpf, J. (2001) Alternative splicing in the ligand binding domain of mouse apoE receptor-2 produces receptor variants binding reelin but not α 2-macroglobulin. *J. Biol. Chem.* **276**, 22160–22169
32. Koch, S., Strasser, V., Hauser, C., Fasching, D., Brandes, C., Bajari, T. M., Schneider, W. J., and Nimpf, J. (2002) A secreted soluble form of apoE receptor 2 acts as a dominant-negative receptor and inhibits reelin signaling. *EMBO J.* **21**, 5996–6004
33. Li, Y., Lu, W., Marzolo, M. P., and Bu, G. (2001) Differential functions of members of the low density lipoprotein receptor family suggested by their distinct endocytosis rates. *J. Biol. Chem.* **276**, 18000–18006
34. Fuentealba, R. A., Barría, M. I., Lee, J., Cam, J., Araya, C., Escudero, C. A., Inestrosa, N. C., Bronfman, F. C., Bu, G., and Marzolo, M. P. (2007) ApoER2 expression increases A β production while decreasing amyloid precursor protein (APP) endocytosis: possible role in the partitioning of APP into lipid rafts and in the regulation of γ -secretase activity. *Mol. Neurodegener.* **2**, 14
35. Christensen, E. I., and Willnow, T. E. (1999) Essential role of megalin in renal proximal tubule for vitamin homeostasis. *J. Am. Soc. Nephrol.* **10**, 2224–2236
36. Bu, G., and Schwartz, A. L. (1998) Rap, a novel type of ER chaperone. *Trends Cell Biol.* **8**, 272–276
37. Andersen, O. M., Benhayon, D., Curran, T., and Willnow, T. E. (2003) Differential binding of ligands to the apolipoprotein E receptor 2. *Biochemistry* **42**, 9355–9364
38. Sun, X. M., and Soutar, A. K. (1999) Expression *in vitro* of alternatively spliced variants of the messenger RNA for human apolipoprotein E receptor-2 identified in human tissues by ribonuclease protection assays. *Eur. J. Biochem.* **262**, 230–239
39. Brown, M. S., Anderson, R. G., and Goldstein, J. L. (1983) Recycling receptors: the round-trip itinerary of migrant membrane proteins. *Cell* **32**, 663–667
40. Beglova, N., Jeon, H., Fisher, C., and Blacklow, S. C. (2004) Cooperation between fixed and low pH-inducible interfaces controls lipoprotein release by the Ldl receptor. *Mol Cell* **16**, 281–292
41. Baker, R. D., Baker, S. S., LaRosa, K., Whitney, C., and Newburger, P. E. (1993) Selenium regulation of glutathione peroxidase in human hepatoma cell line Hep3b. *Arch. Biochem. Biophys.* **304**, 53–57
42. Saito, Y., Hayashi, T., Tanaka, A., Watanabe, Y., Suzuki, M., Saito, E., and Takahashi, K. (1999) Selenoprotein P in human plasma as an extracellular phospholipid hydroperoxide glutathione peroxidase: isolation and enzymatic characterization of human selenoprotein P. *J. Biol. Chem.* **274**, 2866–2871
43. Bosschaerts, T., Guillems, M., Noel, W., Hérin, M., Burk, R. F., Hill, K. E., Brys, L., Raes, G., Ghassabeh, G. H., De Baetselier, P., and Beschin, A. (2008) Alternatively activated myeloid cells limit pathogenicity associated with african trypanosomiasis through the IL-10 inducible gene selenoprotein P. *J. Immunol.* **180**, 6168–6175
44. Ma, S., Hill, K. E., Burk, R. F., and Caprioli, R. M. (2003) Mass spectrometric identification of N- and O-glycosylation sites of full-length rat selenoprotein P and determination of selenide-sulfide and disulfide linkages in the shortest isoform. *Biochemistry* **42**, 9703–9711
45. Chittum, H. S., Himeno, S., Hill, K. E., and Burk, R. F. (1996) Multiple forms of selenoprotein P in rat plasma. *Arch. Biochem. Biophys.* **325**, 124–128
46. Beffert, U., Weeber, E. J., Durudas, A., Qiu, S., Masiulis, I., Sweatt, J. D., Li, W. P., Adelman, G., Frotscher, M., Hammer, R. E., and Herz, J. (2005) Modulation of synaptic plasticity and memory by reelin involves differential splicing of the lipoprotein receptor apoER2. *Neuron* **47**, 567–579
47. Duit, S., Mayer, H., Blake, S. M., Schneider, W. J., and Nimpf, J. (2010) Differential functions of apoER2 and very low density lipoprotein receptor in reelin signaling depend on differential sorting of the receptors. *J. Biol. Chem.* **285**, 4896–4908